Optical Characteristic and Numerical Study of Gold Nanoparticles on Al_2O_3 coated Gold Film for Tunable Plasmonic Sensing Platforms

Chatdanai Lumdee,[†] Binfeng Yun,[†,I] and Pieter G. Kik[*,†,‡]
[†]CREOL, the College of Optics and Photonics; [‡]Physics Department,
University of Central Florida, 4000 Central Florida Blvd, Orlando, FL 32816
[I]Advanced Photonics Center, School of Electronic Science and Engineering, Southeast University,
Nanjing 210096, China

ABSTRACT

Substrate-based tuning of plasmon resonances on gold nanoparticles (NP) is a versatile method of achieving plasmon resonances at a desired wavelength, and offers reliable nanogap sizes and large field enhancement factors. The reproducibility and relative simplicity of these structures makes them promising candidates for frequency-optimized sensing substrates. The underlying principle in resonance tuning of such a structure is the coupling between a metal nanoparticle and the substrate, which leads to a resonance shift and a polarization dependent scattering response. In this work, we experimentally investigate the optical scattering spectra of isolated 60 nm diameter gold nanoparticles on aluminum oxide (Al_2O_3) coated gold films with various oxide thicknesses. Dark-field scattering images and scattering spectra of gold particles reveal two distinct resonance modes. The experimental results are compared with numerical simulations, revealing the magnitude and phase relationships between the effective dipoles of the gold particle and the gold substrate. The numerical approach is described in detail, and enables the prediction of the resonance responses of a particle-on-film structure using methods that are available in many available electromagnetics simulation packages. The simulated scattering spectra match the experimentally observed data remarkably well, demonstrating the usefulness of the presented approach to researchers in the field.

Keywords: coupling simulation, gold resonance, particle-on-film, single particle resonance, substrate coupling

1. INTRODUCTION

Surface plasmon resonances of metallic nanoparticles on polarizable substrates represent one of the most broadly studied platforms for achieving controlled plasmon resonance wavelengths.[1] The particle-on-film structure has been proven to provide a wide resonance tuning range and demonstrated as a potential candidate for many applications, including photovoltaics[2] and sensing.[3,4] The tunability of the plasmon resonance response is the result of the coupling between a metal nanoparticle and a nearby substrate,[5] often referred to as the result of dynamic image charge formation in the substrate underneath the nanoparticle. The plasmon wavelength is known to be controllable by varying the spacing between the nanoparticles and the substrate,[6,7] similar to the observed plasmon resonance shifts of nanoparticle dimer systems as a function of inter-particle separation.[8]

In this study, we present an investigation of the plasmon resonances of 60 nm diameter gold nanoparticles on Al_2O_3 coated gold film. The resonances are controlled using the thickness of the Al_2O_3 coating. The coupling between the nanoparticle and the substrate was modeled using numerical simulation. The simulations reproduce the resonance tuning of the nanoparticles on different Al_2O_3 coated substrates and reveal the polarization dependent coupling responses of the effective dipole moments of the nanoparticle and the underlying gold substrate. The numerical study supports the experimental observations and explains the ring-shaped scattering images of individual nanoparticles. The numerical approach presented in this work could be useful as an accessible method for calculating plasmonic responses of various single-particle-on-film systems.

[*] kik@creol.ucf.edu, phone 1-407-823-4622

Plasmonics: Metallic Nanostructures and Their Optical Properties XI, edited by Mark I. Stockman,
Proc. of SPIE Vol. 8809, 88091S · © 2013 SPIE · CCC code: 0277-786X/13/$18 · doi: 10.1117/12.2024670

2. EXPERIMENTS

2.1 Experimental method

Gold films with 50 nm thickness were deposited on glass cover slips with a 2 nm Cr wetting layer by thermal evaporation using an Edward FL 400 thermal evaporator. In the last deposition step, a thin aluminum film was deposited on top of the gold films without breaking the vacuum (base pressure < 10^{-5} mbar). The aluminum film becomes oxidized entirely upon exposure to ambient environment and turns into an Al_2O_3 coating. The Al_2O_3 film thickness was characterized using a Woollam M2000 Variable Angle Spectroscopic Ellipsometer. The deposition process was repeated for different gold substrates with similar thickness, while changing the aluminum film thickness. The Al_2O_3 coatings on four gold substrates were found to have a thickness of 1.3 nm, 1.5 nm, 2.2 nm, and 3.4 nm, respectively. Gold nanoparticle colloidal solution (BBInternational) diluted with ethanol to a concentration of 2×10^8 particles/mL with a mean particle diameter of 60.4 ± 2.6 nm was drop coated and left to dry on the Al_2O_3 coated gold substrates.

Darkfield microscopy of nanoparticles on the samples was carried out using an Olympus IX71 inverted microscope equipped with a 50× dark-field objective (UMPlanFL 50× BD, N.A.=0.75) and standard dark-field optics. The darkfield images were recorded with two imaging CCD cameras; a Canon EOS 450D digital camera and a HSi-440C Hyperspectral Imaging System (Gooch & Housego). Single particle spectroscopy was conducted in the same set up but sending the scattering signal to a spectrometer (Horiba Jobin-Yvon iHR320 monochromator with Synapse CCD array). The scattering signals of individual particles were obtained from a ~8×8 μm^2 collection area. In order to obtain a single particle scattering spectrum $I_{sc}(\lambda)$, the collected signal from a particle $I_{NP}(\lambda)$ was measured, the collected signal from a nearby reference collection area $I_{REF}(\lambda)$ was subtracted, and the resulting background corrected signal was divided by the collected lamp spectrum $I_{IN}(\lambda)$, corresponding to the formula $I_{sc}=(I_{NP} - I_{REF})/I_{IN}$. Approximately one hundred single particle spectra were recorded from the Al_2O_3 coated gold substrates, including a reference gold substrate without Al_2O_3 coating.

2.2 Experimental Observation

Figure 1(a, solid lines) shows scattering spectra of single gold nanoparticles on different Al_2O_3 coated gold substrates. The scattering spectra were selected from typical spectra measured in the experiment. The spectra show a clear blueshift upon increasing the Al_2O_3 coating thickness from 0 to 3.4 nm, with the main scattering peak shifting from 690 nm to 610 nm. In addition to the main scattering peak, there is a weak resonance peak ~550 nm present in all scattering spectra. Figure 1 (b) and (c) show two columns of dark-field microscopy images of the same gold nanoparticle from each substrate recorded with a Canon EOS 450D digital camera and a HSi-440C Hyperspectral Imaging System, respectively. To construct the images in Fig. 1(c), the HSi-440C recorded a set of spectral images of each nanoparticle then the spectral images were combined into a single false-color image. The color bar represents the false-color function as a function of wavelength The processed images help distinguish nanoparticles scattering responses that have similar resonance wavelengths (down to 5 nm spectral resolution) that could not be distinguished using a conventional RGBcamera. Note that the images in Fig. 1(c) show dumbbell-shaped scattering patterns instead of the ring-shaped scattering patterns shown in Figure 1(b). This is the result of the known polarization dependent response of the HSi-440C.

Figure 1(b) and (c) show ring/dumbbell-shaped scattering patterns of single nanoparticles on different substrates. Among these images only Figures 1(b-i) present a clear central scattering signal at green wavelengths (real color image), while its corresponding scattering spectrum suggests the presence of strong scattering at red/NIR wavelengths. This is the result of a drop in transmission of IR cut filters in the Canon camera (T < 0.1 for wavelength longer than 680 nm). The observations in Fig. 1 indicate the co-existences of two resonance modes, lateral and vertical dipole modes. The origin of these two modes will be discussed in the following section.

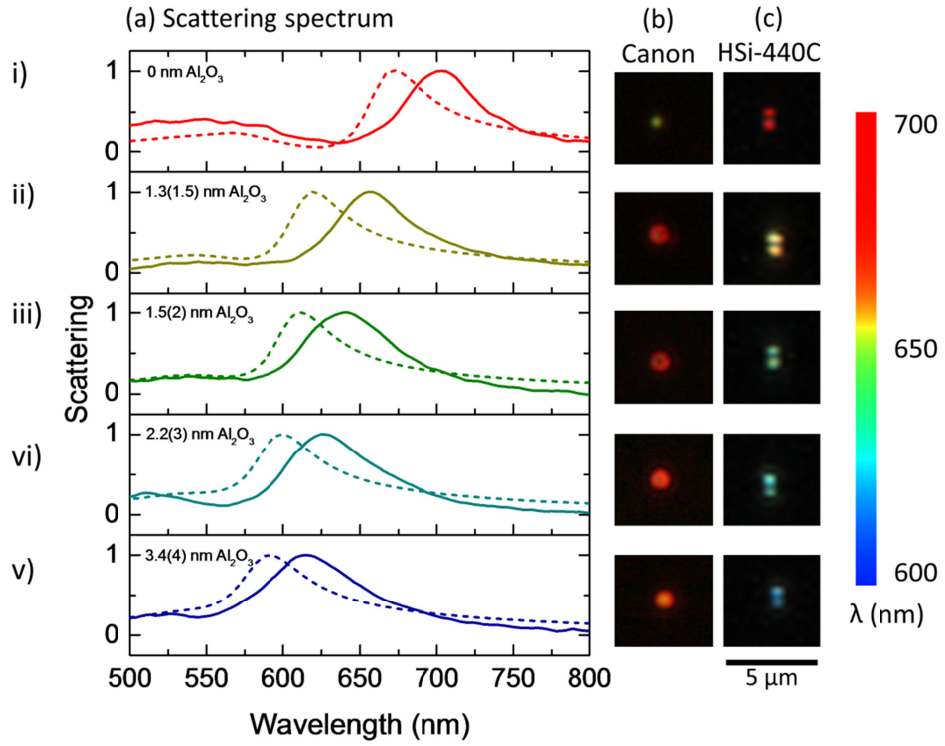

Figure 1. Measured (solid) and calculated (dashed) scattering spectra of a gold nanoparticle on Al_2O_3 coated gold substrates with different Al_2O_3 thicknesses (a). The thicknesses used in the simulation are listed in parentheses. Five pairs of darkfield images of single nanoparticles on different substrates taken with a Canon EOS 450D (b) and a HSi-440C Hyperspectral Imaging System (c). The color bar represents the wavelength color scale used to construct the spectral images in (c).

3. NUMERICAL SIMULATION

3.1 Simulation Model and Calculation Method

Electromagnetic simulation of the structure used in the experiment was performed using CST Microwave Studio.[9] Figure 2 presents the simulated structure consisting of a 60 nm diameter gold nanoparticle placed on an Al_2O_3 coated gold film, with a gold thickness of 50 nm and varying Al_2O_3 thickness to capture the trends observed in the experiments. Material data of gold and Al_2O_3 were taken from Ref. 10 and 11, respectively. To take into account the presence of organic ligands on the gold nanoparticles after deposition from colloidal solution, the gold nanoparticle was coated with a 1 nm thick organic shell of (n = 1.5) in the simulations. A 200 nm unit cell boundary was used in the simulations to avoid reflections from any substrate edges. This gives reliable results as long as particle-particle interactions are minimal in the simulation. The particle is excited with a plane wave arriving at 77° to the substrate surface normal. The incident angle was chosen to be the same as the darkfield illumination angle used in the experiment. Both TE and TM excitation conditions were simulated.

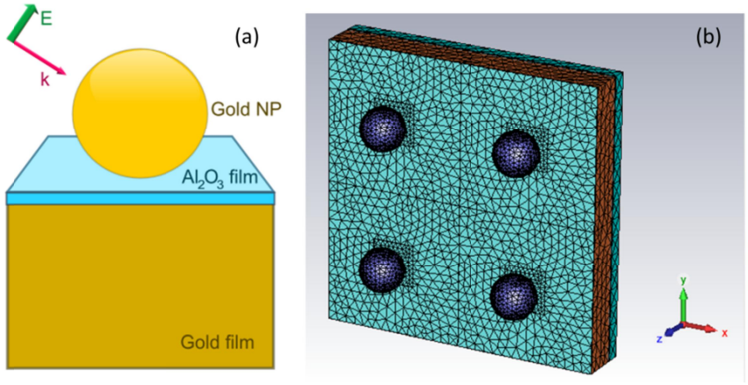

Figure 2. The schematic of the simulated structure used in the simulation (a). The tetrahedral meshes of the simulation structure with the unit cell boundary used in the software (b).

The scattering spectra were calculated based on the simulated field distributions using a simple integrated dipole scattering assumption. First, the effective dipole moment of the nanoparticle (μ_{NP}) and the effective dipole moment of the gold film (μ_{Au}) directly underneath the particle were obtained separately by a volume integration of the particle and substrate polarization (P). The substrate polarization was considered underneath the nanoparticle within a square area as shown by the fine mesh near the particle in Fig. 2(b). The effective dipole moment of the gold film in this same area but in the absence of a particle was subtracted from the data to avoid taking into account substrate response contributions that produce specular reflection as opposed to scattering. The scattering spectrum was then calculated using the total effective dipole moment of the particle-on-film system ($\mu_{total} = \mu_{NP} + \mu_{Au}$) giving the scattering power that is proportional to $|\mu_{total}|^2 \omega^4$.[12] In Figure 1(a) (dashed lines), the calculated scattering spectra of the gold nanoparticle on an Al_2O_3 gold film with different Al_2O_3 thickness were plotted, showing a similar tuning response as a function of Al_2O_3 thickness as observed in experiments.

4. RESULTS AND DISCUSSION

As previously mentioned the observed resonance modes and their spectral response will be explained by comparing with the simulation results. Figure 3 presents the effective dipole moment magnitude and phase of the nanoparticle and the underlying gold film from the simulation with 1.5 nm Al_2O_3 thickness. Two components are shown, the lateral dipole moment under TE plane wave excitation and the vertical dipole moment under TM plane wave excitation.

In Figure 3(a), the magnitude of the effective dipole moments of both the nanoparticle (solid lines) and the gold film (dashed lines) are seen to have a strong vertical dipole moment (red) and a weaker lateral dipole moment (blue). The ratio between the maximum value of the nanoparticle dipole moment magnitude and the gold film dipole moment magnitude of the lateral and the vertical modes are 3.37 and 2.38, respectively. If ones consider only the nanoparticle dipole moment without taking into account the substrate contribution, the calculated scattering signal shows noticeable differences compared to the features found in the experiment. The main difference is that the calculated scattering spectrum has a stronger peak as the short wavelength (~550 nm) compared to that of the measured spectrum. The differences between the simple scattering spectrum calculation and the experimental results are reduced when taking into consideration the effective dipole moment of the gold film underneath the particle. Figure 3(b) reveals the phase relationship between the two effective dipole moments (that of the particle and the substrate) of the two resonance modes. The plot indicates a clear difference between the lateral and the vertical resonance modes. The lateral dipoles of the nanoparticle and the gold film are seen to be out of phase across the entire wavelength range of interest while the vertical dipole moments stay in-phase. These factors result in a strong vertical scattering component at long wavelength and a reduced lateral scattering component of the gold nanoparticle on Al_2O_3 coated gold films, as also observed in the measure spectra.

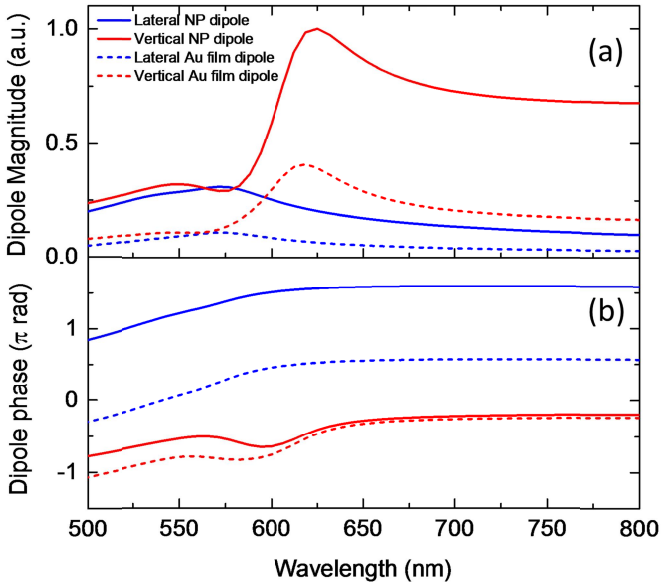

Figure 3. The effective lateral and vertical dipole moment magnitude (a) and phase (b) of the gold nanoparticle and the gold film upon excitation with TE and TM waves, respectively.

Figure 4 presents the dark field scattering images of a gold nanoparticle on an Al_2O_3 coated gold film with a 1.5 nm Al_2O_3 thickness (same as Figure 1 row ii). The top row shows a schematic drawing of how scattering associated with the lateral and the vertical resonance modes are collected by the objective lens and the CCD cameras. Image dipoles in the gold substrate are drawn schematically with the respective phases to the nanoparticle dipoles as found in the numerical simulation results shown in Figure 3. The middle and the bottom rows show the combined and separated images corresponding to the two scattering image modes of the same particle recorded with a Canon EOS 405D digital camera and a HSi-440C Hyperspectral Imaging System, respectively. The decomposed images were converted to gray-scale to facilitate a comparison between the scattering patterns of the two modes. The right column represents the scattering of the stronger peak of the scattering spectrum which is seen to show a clear evidence of the vertical dipole modes (ring/dumbbell shaped). The weak lateral dipole mode was enhanced (the Red signal of the RGB camera was removed/only a spectral image at 550 nm from the Hyperspectral camera was selected, the brightness and contrast were adjusted) to highlight the difference in scattering pattern for the resonance modes in this particle-on-film plasmonic system. The short-wavelength scattering pattern shows a central scattering spot similar to the observation in Figure 1(b) row i, where the long wavelength response was cut by the Canon camera transmission window. The experimental observations closely match the expectations based on the simulated dipole moments of the nanoparticle and the induced dynamic image charge in the substrate, providing a clear explanation of the development of the distinct scattering patterns commonly observed in single particle spectroscopy studies of particle-on-film structures.

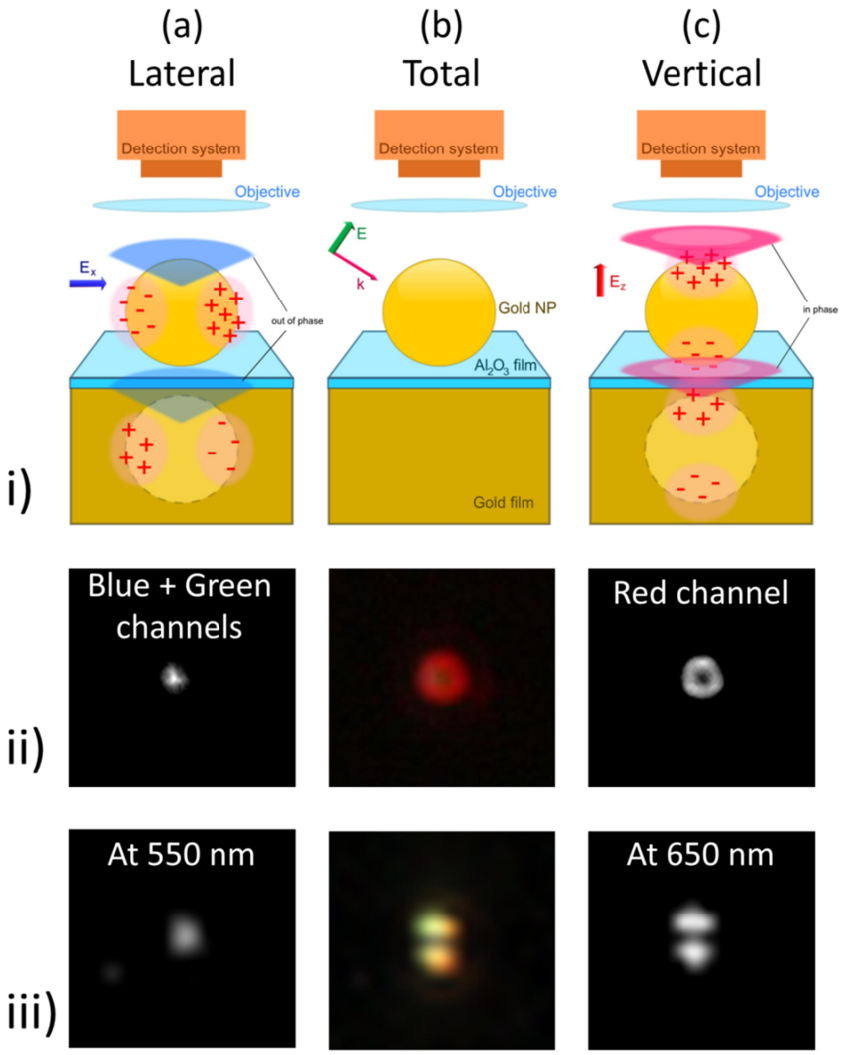

Figure 4. Row i) Schematic representations (top row) of the coupling between the gold nanoparticle and the gold film in the presence of a 1.5 nm thick Al_2O_3 spacer layer due to the formation of dynamic image charges, showing separately the lateral (left column) and the vertical (right column) charge motion and corresponding scattering patterns collected by the digital RGB camera (second row) and the spectral imaging system (third row). The central column represents the composite data under dark-field illumination resulting in the simultaneous excitation of both lateral and vertical dipole moment.

5. CONCLUSION

Plasmon resonance modes of a gold nanoparticle on an Al_2O_3 coated gold film are investigated as a model for the interactions occurring in particle-on-film plasmonic structures. The scattering spectra of gold nanoparticles show a blueshift of the scattering signal originating from a vertical dipole moment from 690 nm to 610 nm as the Al_2O_3 layer thickness increases from 0 to 3.4 nm. The scattering peak associated with a lateral oscillatory dipole moment stays independent of the Al_2O_3 thickness at ~ 550 nm. The characteristic of the two resonance modes emerges from the difference in coupling between the effective dipole moments of the nanoparticle and the gold film when the particle is excited by light with different polarization directions. Numerical simulations show that the lateral dipole moment of the nanoparticle and the gold film have a ~180° phase difference, causing a weak net dipole and weak scattering in the short wavelength region. The vertical dipoles on the other hand are almost perfectly in phase, resulting in a strong plasmon resonant scattering signal in the long wavelength region. Decomposed darkfield images visually demonstrate the co-existence of the two resonance modes and their scattering patterns, and how the scattering is projected to the CCD

cameras. The study explicitly demonstrates the origin of the characteristic particle appearance in scattering images and relative peak strength in scattering spectra of metal-particle-on-film structures. In addition, the method is based on a simple dipole integration technique facilitated by numerical simulation software which is easy to implement.

REFERENCES

[1] Halas, N. J., Lal, S., Chang, W. S., Link, S. and Nordlander, P., "Plasmons in Strongly Coupled Metallic Nanostructures," Chem Rev 111(6), 3913-3961 (2011).

[2] Mokkapati, S., Beck, F. J., de Waele, R., Polman, A. and Catchpole, K. R., "Resonant nano-antennas for light trapping in plasmonic solar cells," J Phys D Appl Phys 44(18), 185101.1-185101.9 (2011).

[3] Mubeen, S., Zhang, S. P., Kim, N., Lee, S., Kramer, S., Xu, H. X. and Moskovits, M., "Plasmonic Properties of Gold Nanoparticles Separated from a Gold Mirror by an Ultrathin Oxide," Nano Lett 12(4), 2088-2094 (2012).

[4] Li, L., Hutter, T., Steiner, U. and Mahajan, S., "Single molecule SERS and detection of biomolecules with a single gold nanoparticle on a mirror junction," The Analyst 138(16), 4574-4578 (2013).

[5] Knight, M. W., Wu, Y. P., Lassiter, J. B., Nordlander, P. and Halas, N. J., "Substrates Matter: Influence of an Adjacent Dielectric on an Individual Plasmonic Nanoparticle," Nano Lett 9(5), 2188-2192 (2009).

[6] Mock, J. J., Hill, R. T., Degiron, A., Zauscher, S., Chilkoti, A. and Smith, D. R., "Distance-Dependent Plasmon Resonant Coupling between a Gold Nanoparticle and Gold Film," Nano Lett 8(8), 2245-2252 (2008).

[7] Hutter, T., Elliott, S. R. and Mahajan, S., "Interaction of metallic nanoparticles with dielectric substrates: effect of optical constants," Nanotechnology 24(3), 035201.1-035201.8 (2013).

[8] Nordlander, P. and Prodan, E., "Plasmon hybridization in nanoparticles near metallic surfaces," Nano Lett 4(11), 2209-2213 (2004).

[9] CST MICROWAVE STUDIO®, Computer Simulation Technology, Darmstadt, Germany, (2012).

[10] Johnson, P. B. and Christy, R. W., "Optical Constants of the Noble Metals," Phys Rev B 6(12), 4370-4379 (1972).

[11] Palik, E. D. and Ghosh, G., [Handbook of Optical Constants of Solids], Academic Press, Orlando; London, (1985).

[12] Jackson, J. D., [Classical Electrodynamics], Wiley, New York, (1962).